Resonant Meta-Surface Superstrate for Single and Multifrequency Dipole Antenna Arrays

Elena Sáenz, *Student Member, IEEE*, Ramón Gonzalo, *Member, IEEE*, Iñigo Ederra, John C. Vardaxoglou, *Member, IEEE*, and Peter de Maagt, *Fellow, IEEE*

***Abstract*—The design of a multifrequency dipole antenna array based on a resonant meta-surface superstrate is proposed. The behavior of a single element that is closely placed to a meta-surface is experimentally investigated. The proposed meta-surface is based on resonating unit cells formed by capacitively loaded strips and split ring resonators. By tuning a dipole antenna to the pass band of the meta-surface, the physical area is effectively illuminated enhancing the radiation performance. The gain, radiation efficiency and effective area values of the whole configuration are compared to the ones obtained with a single dipole without superstrate. Radiation efficiency values for the proposed configuration of more than 80% and gain values of more than 4.5 $\pm$1 dB are obtained. Based on this configuration, simulated results of a multifrequency antenna array are presented. Distinctive features of this configuration are high isolation between elements (20 dB for a distance of $\lambda_0/4$), and low back radiation.**

***Index Terms*—Effective area, meta-surfaces and multifrequency arrays, metamaterials.**

I. Introduction

SINCE THE eighties, the resonance method to improve the gain of printed antennas has been well documented [1]–[3]. This method is based on the addition of a superstrate or cover layer with either $\varepsilon \gg 1$ or $\mu \gg 1$ over the substrate. By appropriately choosing the layer thickness and the dipole position, relatively large gain may be realized. In [2], [3], the resonance gain conditions and asymptotic formulas for resonance gain, beamwidth and bandwidth (BW) were investigated. In those papers gain and radiation resistance are substantially improved over a significant BW. Nevertheless, these configurations require fairly thick layers, about $\lambda/2$ in the media, leading to an overall thickness which could be incompatible with integrated circuit antenna applications in most of the cases. Besides, the BW varies inversely with gain so that a moderate gain limit is established for practical antenna operation and therefore the design becomes more sensitive to the device parameters. Furthermore, the aperture efficiency of those configurations is typically less than 60%.

Recently, several authors have proposed the application of electromagnetic band gap (EBG) structures [4]–[12] as superstrates in order to improve the antenna performances. Typically, an EBG array which consists of dielectric elements and characterized by stop/pass bands is employed as a cover for antennas to enhance the gain of a single patch antenna. The EBG acts equivalent to an aperture antenna and its effective aperture size becomes larger than that the original feeding antenna. The issue of thickness remains as the period of the EBG structure is close to $\lambda/2$ and more than one period is needed over the single antenna. However, aperture efficiencies close to 80% are obtained [11], [12]. Frequency selective surfaces (FSS) [13] based on the Fabry-Perot effect [14] have also been proposed as an alternative to dielectric EBGs for gain enhancement. The FSS offers similar transmission and reflection characteristics, but is thinner than the EBG configuration. However, the distance between the FSS superstrate and the ground plane of the antenna, which determines the resonant frequency, still needs to be about $\lambda_0/2$ of the resonant frequency of the resonator.

More recent results proposed in [15]–[17] have used either artificial magnetic conductor (AMC) surfaces or metamaterial ground planes (MPG) in combination with partially reflective surfaces (PRS) to design low-profile high-gain planar antennas. The overall thickness of the configuration has been reduced to $\lambda_0/6$ and the aperture efficiency rounds to 60%.

In [18], artificial dielectrics realized as arrays of thin conducting wires periodically loaded by reactive impedances (capacitances) are presented. This artificial structure allows the array period to be reduced although the wire medium is restricted to operation at low frequencies. The artificial lens properties of this structure can in principle be electrically regulated by controlling load reactances, with the main advantage of the possibility to realize electrical scanning. However, if only capacitively loaded wires are used in the lattice, manufacturing tolerances remain an issue of concern. This configuration has been proposed to base-station antennas [18].

Recently, metamaterial (MTM) structures have shown their benefits as superstrate of planar antennas [19]–[22]. This paper proposes the use of meta-surfaces on top of dipole antenna arrays in order to improve their radiation performance. For a single element, the main advantages which are derived from this work are the compactness (total thickness less than $\lambda_0/4$), and the high radiation efficiency (around 80%). These

Manuscript received August 7, 2007; revised November 22, 2007. This work was supported by the METAMORPHOSE NoE funded by the EU under Contract NMP3-CT-2004-50252 and the Spanish Government under project TEC2006-13248-C04-03/TCM.

E. Saenz, R. Gonzalo, and I. Ederra are with the Antenna Group, Public University of Navarra, 31006 Pamplona, Spain (e-mail: ramon@unavarra.es).

J. C. Vardaxoglou is with the Department of Electronic and Electrical Engineering, Loughborough University of Technology, Loughborough LE11 3TU, U.K. (e-mail: J.C.Vardaxoglou@lboro.ac.uk).

P. de Maagt is with the European Space Research and Technology Centre (ESTEC), European Space Agency, 2200 AG Noordwijk, The Netherlands (e-mail: Peter.de.Maagt@esa.int).

Color versions of one or more of the figures in this paper are available online at http://ieeexplore.ieee.org.

Digital Object Identifier 10.1109/TAP.2008.919212

meta-surfaces are based on resonant cells [23]–[25], which exhibit pass band and stop band properties at which the power is transmitted or reflected respectively. Due to their resonant behavior, it is possible to design superstrates resonating at a different frequency resulting in low coupling between them. This fact is used to create a compact multifrequency dipole antenna array with short distance between dipoles, less than $0.3\lambda_0$, and good level of isolation.

The first part of this paper, Section II, is focused on an alternative technology of superstrates based on the use of meta-surfaces. The unit cell selected to create the meta-surface superstrate, the manufacturing process and the resonant frequency measured under waveguide excitation are presented. The radiation performance of the superstrate while fed with a dipole is assessed in Section III. Measurements of the S_{11} parameter, the resonant frequency, the gain and the radiation pattern have been carried out for different geometrical sizes of the superstrate, i.e., varying the number of unit cells. Using these measurements, the radiation efficiency and the effective area have been derived. Moreover, the radiation efficiency has also been obtained independently using the Wheeler cap method and compared with the one obtained by the pattern integration technique. Both results are in good agreement. In Section IV the main advantages of the proposed configuration are stressed and the design of a multifrequency dipole antenna array is outlined. The work is concluded in Section V.

II. Meta-Surface Design

During the recent years, several double negative materials (DNG) have been designed by different authors [23]–[25] several of them based on the topology proposed by [26], i.e., a combination of split ring resonators (SRRs) and wires. In order to correctly excite the "SRR/wire" unit cells, a plane wave with the E-field parallel to the wires and H-field axial to the SRR is required, which means a propagation vector parallel to the SRR plane.

In this work, the meta-surface under study is based on the unit cell proposed by Prof. Ziolkowski in [25]. Although this unit cell presents double negative (DNG) behavior, i.e., negative refractive index, at a certain frequency band, in this paper its resonance transmission effect at the frequency band of positive refractive index is used. Since the role of the DNG behavior is not exploited, the terminology meta-surface will be used. The unit cell is constituted by a dielectric slab in which four capacitively loaded strips (CLSs) and one SRR are embedded (see Fig. 1).

To construct the unit cell, a layer by layer technique described in detail in [19]–[21] is followed. The material selected to fabricate the layers was RT/Duroid 5880, a low loss dielectric characterized by the parameters $\varepsilon_r = 2.2$, loss tangent $tan\delta = 0.0009$, thickness 0.254 mm and copper cladding 70 μm on both faces. Three different types of layers (1, 2 and 3) were required to create the meta-surface unit cell. One period is constructed (see Fig. 1(b)), by stacking the layers following the pattern 123321.

The transmission and reflection properties of the manufactured meta-surface were tested under waveguide excitation. A media which consists on 12×4 unit cells in the transversal directions and 1 in the propagation one was placed in between two

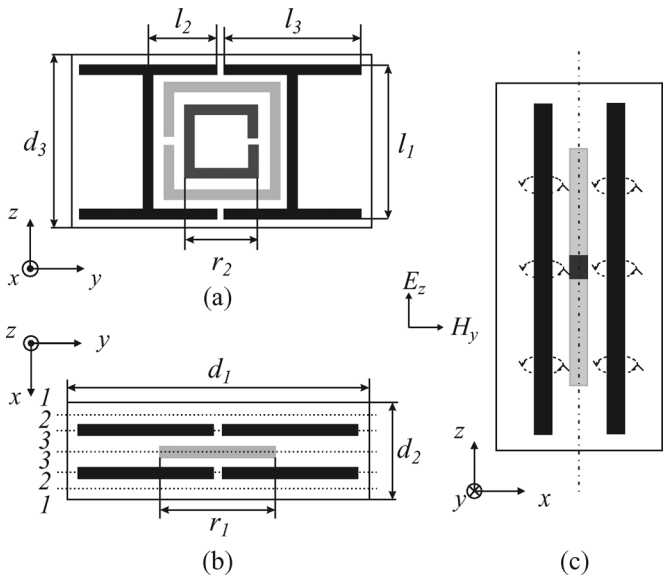

Fig. 1. Geometry of the unit cell. Width of all the gaps and lines $= 0.254$ mm, $d_1 = 7.366$ mm, $d_2 = 1.944$ mm, $d_3 = 4.318$ mm, $l_1 = 3.81$ mm, $l_2 = 1.778$ mm, $l_3 = 3.556$ mm, $r_1 = 2.794$ mm, $r_2 = 1.778$ mm. (a) Front view. (b) Top view. The three types of layers (1, 2 and 3) are marked. (c) Cancellation of the currents in the symmetric plane.

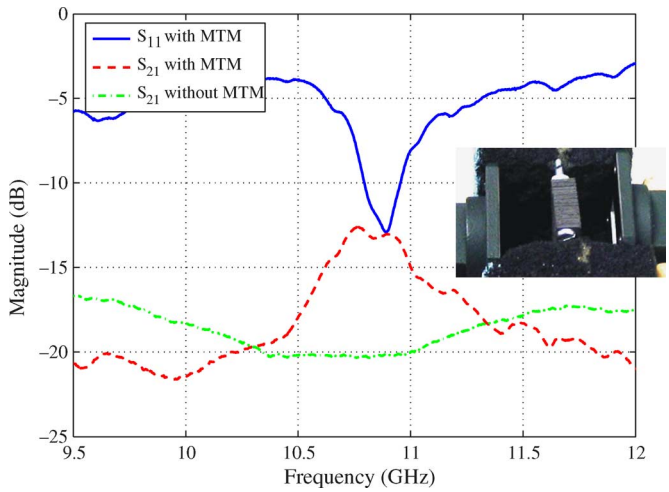

Fig. 2. Transmission and reflection properties of the meta-surface under waveguide excitation. Inset: set-up for the measurements; the metamaterial is placed in between the waveguides.

WR75 rectangular waveguides (19×9.5 mm) (see inset Fig. 2). The measured results are depicted in Fig. 2. Comparing the S_{21} parameter between waveguides with and without the metamaterial, an enhancement of 8 dB is obtained around the resonant frequency of 10.9 GHz.

III. Radiation Performance

As was mentioned before, this meta-surface is basically a resonant structure exhibiting pass and stop bands. It is formed by a finite periodic repetition of the unit cell. The key idea behind this configuration is to allow radiation from a primary source to spread over a larger radiating aperture. By tuning a dipole antenna to the pass band frequency of the superstrate, an in-phase resonance of the unit cells will be induced leading to a more uniform illumination of the superstrate. So, the radiating effective

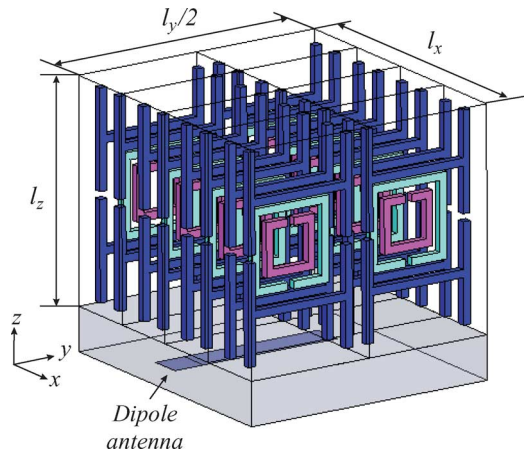

Fig. 3. Configuration of the dipole antenna with the 4 × 4 uniform superstrate. Notice that electromagnetic symmetry properties were applied on the xz plane, so only half of the structure is shown. Total dimensions: $l_x = 0.31\lambda_0$, $l_y = 0.58\lambda_0$, $l_z = 0.25\lambda_0$.

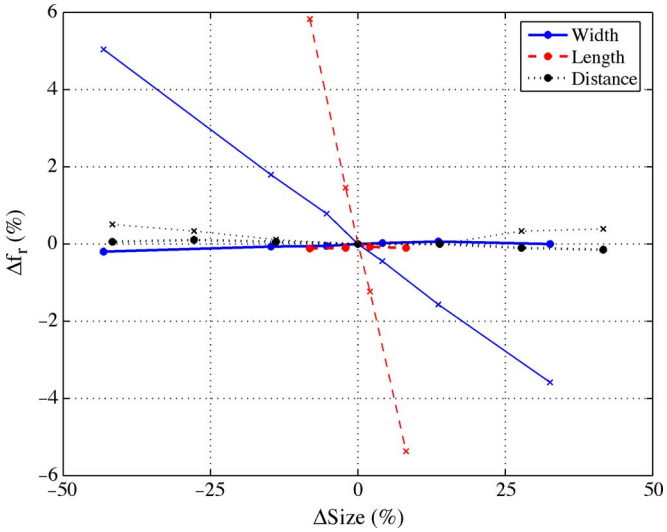

Fig. 4. Deviation of the resonant frequency of the dipole with meta-surface (thick line) and without it (thin line) with respect to the optimized configuration when the width and length of the dipole and the distance from the dipole to the superstrate are modified in comparison with the optimum ones: $\text{width} = 1.05\ \text{mm}$, $\text{length} = 9.8\ \text{mm}$, $\text{distance} = 0.72\ \text{mm}$.

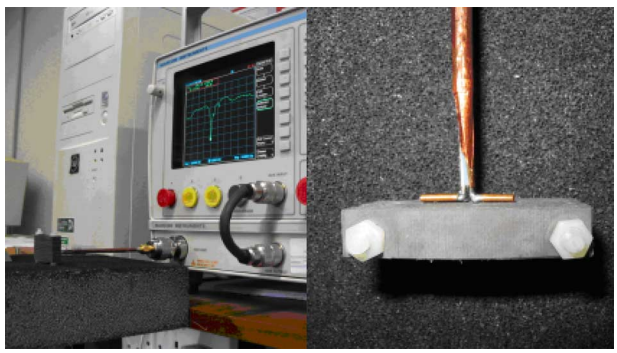

Fig. 5. Set-up for the measurements of the S_{11} parameter.

area of the antenna will be enlarged. Once the meta-surface was designed, it was fed by an ideal dipole antenna designed with Ansoft-HFSS. Notice that the overall configuration was optimized with Ansoft-HFSS to obtain the best performances; this includes, the distance between the dipole and the meta-surface, the length of the dipole, the number of periods of the meta-surface, etc.

Fig. 3 shows a sketch of the proposed dipole antenna with an uniform superstrate configuration formed by 4 × 4 cells in the xy plane and 1 period in the z direction. Electromagnetic symmetry properties were applied in order to reduce the computational time, so only half of the structure is shown in this figure. The thickness of the superstrate in the z direction is 7.366 mm (see Fig. 1 caption), i.e., $l_z = \lambda_0/4$, where λ_0 is the free space wavelength at the design resonant frequency of 11.15 GHz. The physical orientation of the dipole with respect to the superstrate is fixed by the requirements of an E-field parallel to the CLSs and an H-field axial to the SRRs in order to correctly excite the cells. The dimensions and position of the dipole were optimized by simulating it embedded in a dielectric slab of $\varepsilon_r = 2.2$ and loaded with the superstrate. The optimum parameters were determined by a good matching and gain enhancement. The final dimensions are: $\text{width of the arms} = 1.05\ \text{mm}$, $\text{length of the arms} = 9.8\ \text{mm}$ and $\text{distance from the antenna to the superstrate} = 0.72\ \text{mm}$. The dipole was fed by and ideal lumped port with an optimized impedance of 51.56 Ω.

After the simulations, an experimental validation of the results was performed. For practical reasons, a $\lambda_0/2$ dipole without ground plane fed by a coaxial balun was used as feeding source instead of the planar printed dipole. The length of the dipole was chosen according to the optimized results. The radius of the arms was around half of the optimized planar ones taking into account the cylindrical shape. In order to estimate the sensitivity of the configuration to small variations in the width and length of the dipole and the distance from the dipole to the superstrate, a sensitivity analysis was performed. Fig. 4 shows the deviation of the resonant frequency of the dipole with and without superstrate with respect to the optimized configuration when the dimensions of the dipole are slightly modified. It is observed that in the presence of the meta-surface, the system is more stable, with a resonant frequency that remains almost constant ($\Delta f_r < 1\%$). In the absence of the meta-surface, for the same variation of the physical dimensions of the dipole, the deviation of the resonant frequency reaches 6%.

In order to determine the level of the improvements in the radiation performance due to the meta-surface, the S_{11} parameter and the radiation pattern of the dipole plus superstrate were measured and, by means of these results, the gain, radiation efficiency and effective area were derived.

A. S_{11} Parameter

The S_{11} parameter of the dipole with the superstrate was measured by using a network analyzer (Marconi 6210 Reflection Analyzer). Based on the simulation optimization process the dipole was placed just above the superstrate. The set-up for the measurements is shown in Fig. 5.

The influence of the meta-surface in the impedance matching of the dipole was analyzed and measured by varying the number of periods of the superstrate in the x direction from 4 to 12.

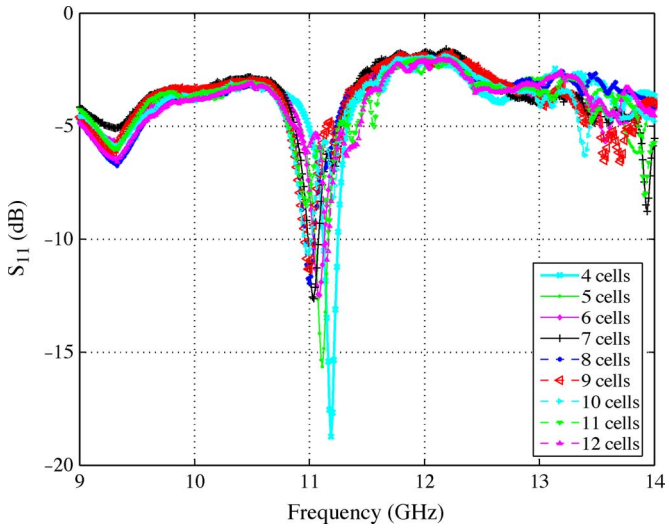

Fig. 6. Magnitude of the S_{11} parameter versus frequency as function of the number of cells as superstrate.

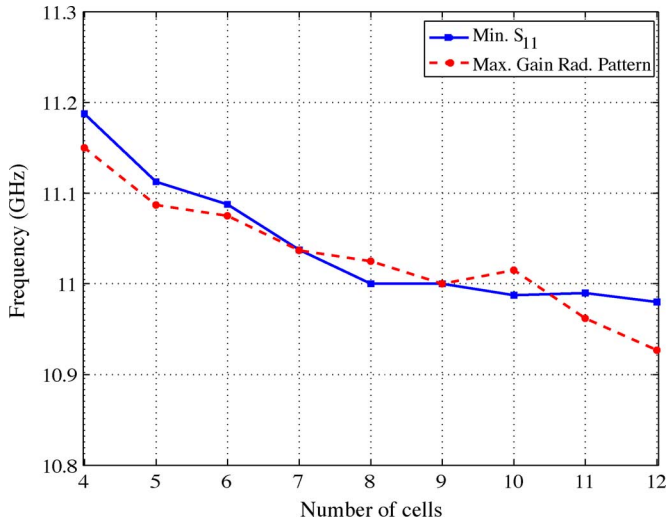

Fig. 7. Resonant frequency versus number of cells.

The magnitude of the S_{11} parameter versus the frequency for all the measured configurations is shown in Fig. 6. As expected, an impedance matching better than -12 dB with a resonant frequency around 11.1 GHz and a deviation smaller than 3.5% with respect to the central frequency has been obtained.

B. Resonant Frequency

Fig. 7 shows the dependence of the resonant frequency (minimum S_{11}) of the configuration (meta-surface + dipole) and the frequency of maximum gain at boresight with the number of cells of the superstrate. The process of deriving the gain will be explained in the next section. It can be observed that both parameters do not exactly coincide, but there is a slight frequency shift between them. This is attributed to errors in the measurements. However, a similar tendency was obtained in both cases; as the number of cells increases, the resonant frequency decreases varying from 11.19 GHz in the case of 4 cells to 10.9 GHz in the case of 12 cells [this agrees with the result obtained with the waveguide measurements (see Fig. 2)]. The resonant frequency curve flattens for larger superstrates since the meta-surface trends to behave as a more uniform media resonating at 10.9 GHz instead of a set of single scatterers.

C. Gain

In order to characterize the different configurations in terms of absolute-gain, the two-antenna method described in [27] was followed.

The gain of the radiating configurations was measured in an anechoic chamber and compared with the one of a single dipole by using a horn antenna as receiver and the dipole (with and without superstrate) as transmitter. The superstrate was placed close to the dipole, as in the case of the S_{11} measurements, in order to maximize the power radiated at boresight. The set-up used for these measurements is shown in Fig. 8.

Placing the horn antenna in front of the dipole + superstrate and analyzing the power received P_R versus the frequency (see Fig. 9), a filtering behavior can be observed due to the pass band

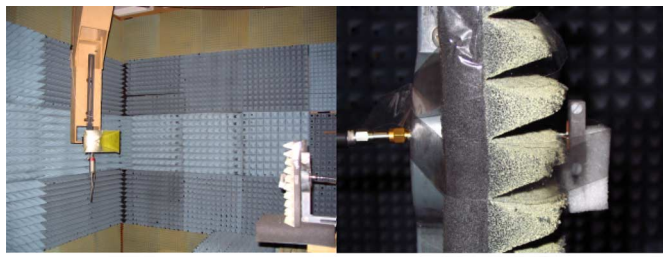

Fig. 8. Set-up for the gain and radiation patterns measurements. (a) Anechoic chamber. (b) Detail of the dipole with the meta-surface.

properties of the superstrate. As in the case of the S_{11}, this relation has been parametrically analyzed by varying the number of cells in the x direction from 4 to 12. Similar results to the one presented in the Fig. 9, which corresponds to the case of a superstrate with nine periods, were obtained for all the cases. Notice that in this case (nine periods), the resonant frequency in terms of minimum S_{11} and maximum gain coincides (see Fig. 7). Comparing the power received with the dipole plus superstrate (dashed line) with the case of the single dipole (continuous line), an improvement of 3.5 dB approximately around the resonant frequency of the superstrate (around 11 GHz) and a rejection larger than -10 dB out this band was achieved. Comparable received and rejected values were obtained for the other configurations.

Measuring the power received P_R at that resonant frequency and taking into account the power transmitted P_T, the gain of the receiver horn antenna G_R for each frequency, the distance between antennas d and the working frequency λ_0, the gain of the transmitting antenna G_T can be calculated by applying the Friis equation as follows:

$$G_T(dB) = 20\log\left(\frac{4\pi d}{\lambda_0}\right) + P_R - P_T - G_R. \qquad (1)$$

Fig. 10 shows the measured gain in the direction of maximum radiation as function of the number of cells. Taking into account

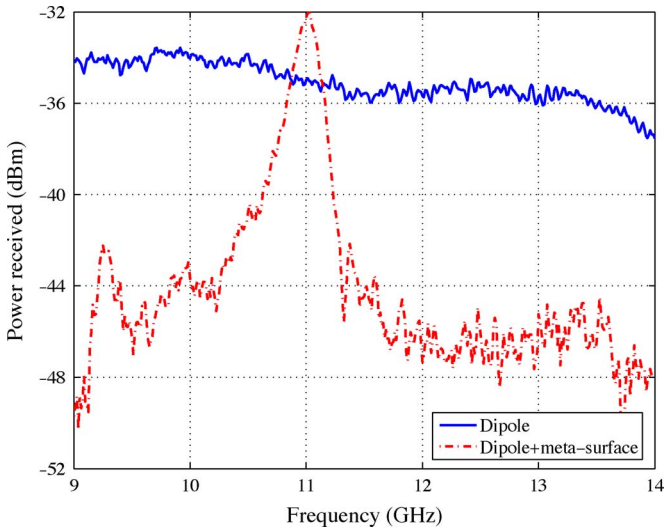

Fig. 9. Power received P_R versus frequency with and without meta-surface for the case of a superstrate that consists of nine periods.

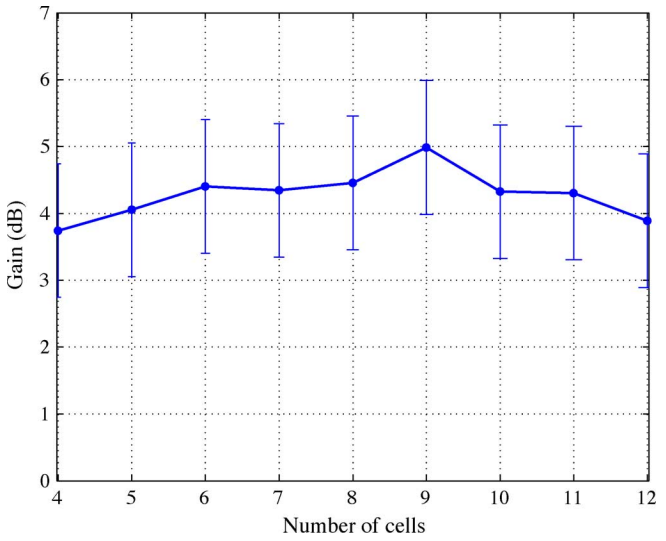

Fig. 10. Measured maximum gain at boresight. Uncertainty in the gain measured estimated to be ± 1 dB.

the errors in calibration, equipment and measurements, the uncertainty in the gain measured is estimated to amount to ± 1 dB. It is also noticeable that the errors increase when low gain antennas are measured. As it was expected, as the number of cells increases, i.e., the radiating surface increases, the gain increases as well. However, a saturation effect can be observed for superstrates with a number of cells between 6 and 11. The reason for this is the appearance of a standing wave in the transversal direction of the configuration, which limits the maximum size of the structure that achieves large gain.

D. Radiation Pattern

Once the frequency of maximum gain was known (see Fig. 9), the radiation patterns were measured at that frequency. In order to avoid reflections from the clamp and the feeding cable, the back side of the antenna was covered with the absorbing material shown in Fig. 8(b). As it is observed, there is a distance between the absorbing material and the dipole, so the distortion in the endfire radiation at $\pm 90°$ is minimum. The back radiation pattern (from 90° to 270°) was not measured because of physical limitations in the test set-up (see the back side feeding network and clamp in Fig. 8). However, the maximum back radiation level was estimated by rotating the antenna 90° and measuring the power received at 270°.

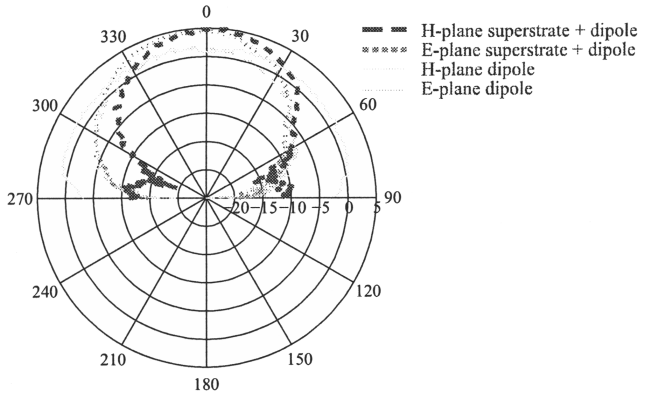

Fig. 11. Gain of the H and E plane radiation patterns for a single dipole and a dipole with superstrate that consists of nine periods.

Fig. 11 shows the H and E-plane radiation patterns for the case of nine cells. Comparing the radiation patterns with and without superstrate, the gain enhancement can be observed. In the case of the H-plane, the omnidirectional radiation pattern for the single dipole becomes more directive when the superstrate is placed on top of it. The H-plane end-fire radiation has been reduced in approximately 15 dB. The back radiation level at 180° was around -5 dB what means a front-back radiation of 10 dB.

E. Radiation Efficiency

The radiation efficiency η_r is defined as the ratio of the total power radiated by the antenna to the total power accepted by the antenna at its terminals during radiation. It can also be defined, as the ratio of the gain to directivity both measured in the direction of maximum radiation (2)

$$\eta_r = \frac{G}{D}. \tag{2}$$

The directivity in the direction of maximum radiation D can be computed (3) by means of the maximum radiation intensity obtained by the measurements $U_{\max}$ and evaluating numerically the power radiated P_{rad} for all the θ and ϕ angles. To do so, the radiation pattern is integrated by sampling the field in the measured H and E planes [27]

$$D = \frac{4\pi U_{\max}}{P_{\text{rad}}}. \tag{3}$$

Since the back radiation pattern was not measured but only the maximum at 180° (-5 dB), a uniform back radiation of -5

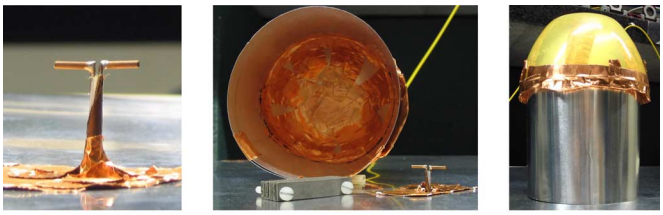

Fig. 12. Set-up for the Wheeler cap measurements. (a) Dipole antenna with the ground plane. (b) Dipole antenna, meta-surface and cap. (c) Cap covering the antenna.

dB was assumed from 90° to 270° in order to not overestimate the radiation performance of the antenna. Although this integration with only two planes gives a rough approximation of the directivity, the result could be considered accurate enough since the radiation patterns are almost symmetrical.

Following this approach, the radiation efficiency has been computed for all the configurations, (see Fig. 13 solid line), taking into account ±1 dB errors in the gain measurements. In the cases of a superstrate with a number of cells from 4 to 10, a flat behavior has been obtained with radiation efficiency values higher than 80%. For superstrates smaller or larger, the radiation efficiency reduces, but it always exceeds 50%.

In order to check that the previous assumptions were correct, the radiation efficiency was also measured by applying the Wheeler cap method [28]. The radiation efficiency is, for this case, defined as

$$\eta_r = \frac{P_R}{P_I} = \frac{P_R}{P_R + P_L} \tag{4}$$

where P_R is the total radiated power, P_I is the total power input, P_L is the total power lost, which includes ohmic losses in the antenna as well as losses in any matching networks considered as part of the antenna.

An equivalent definition of efficiency is given by

$$\eta_r = \frac{R_R}{R_R + R_L} \tag{5}$$

where R_R is the radiation resistance and R_L is the loss resistance. The quantity $R_R + R_L$ is the real part of the antenna input impedance and can be determined from the measurements. Wheeler in [28] reports that enclosing the antenna with a conducting sphere a radian length in radius will eliminate R_R from the input impedance without significantly changing R_L. So, the real part of the input impedance with the sphere in place will be R_L. Thus by making two impedance measurements, without and with the cap, the radiation efficiency can be determined by using (5).

The set-up for the Wheeler cap measurements is shown in Fig. 12. Since a ground plane is required to carry out the measurements, the distance between the ground plane and the dipole was chosen as $\lambda_0/4$ in order to minimize the distortion to the radiation. The cap was a metallic cylinder whose height was approximately the same as its diameter with an spherical cap on top of it [see Fig. 12(b) and (c)]. This way, no extra modes are generated inside the cap, which means the cap is not interfering [28].

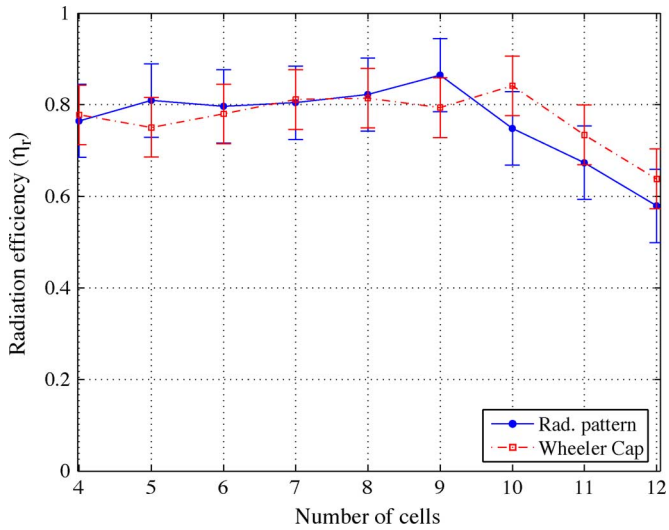

Fig. 13. Radiation efficiency (η_r) versus number of cells. Pattern integration technique and Wheeler cap method.

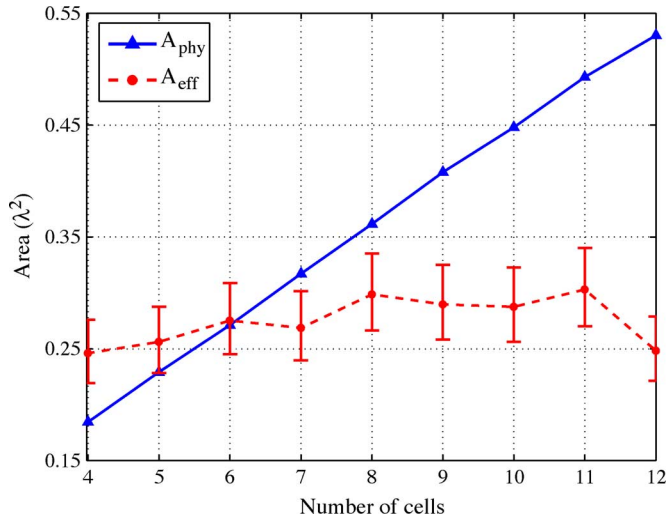

Fig. 14. Physical area (A_{phy}) and effective area (A_{eff}) versus number of cells.

These measurements have been carried out for all the configurations. The results are plotted in Fig. 13 (dashed line) and they are in good agreement with the previous ones calculated by integrating the radiation pattern.

As it was proven in [29], errors around plus or minus 25% can be obtained between the radiation efficiency values when the pattern integration technique is compared with the Wheeler cap method. In order to obtain similar results, identical ground-plane conditions must be kept. In this case, the radiation patterns were measured without ground plane but the Wheeler cap efficiency requires a ground plane. Therefore, slightly different radiation efficiency values have been obtained with both methods. The ground plane effect was also observed in the resonant frequency of the antenna. Although there was 200 MHz frequency shift towards lower frequencies compared to the results presented in Fig. 7, the trend was the same.

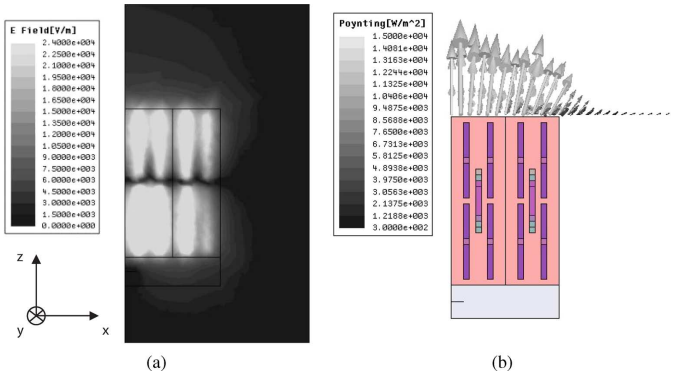

Fig. 15. Superstrate with four cells. Notice that periodic boundary conditions were applied on the xz and yz planes, so only one forth of the structure is shown. (a) E field on the H plane of the dipole (xz) at the resonant frequency 10.8 GHz. (b) Poynting vector on the radiating surface at the resonant frequency.

Using the single dipole as reference case, the radiation efficiencies obtained were 0.86 and 0.73 with the pattern integration technique and Wheeler cap method respectively. That means an error of around 17% between the two methods, what is within expectations.

F. Effective Area

Once the maximum directivity at boresight D of the configuration is obtained, the effective area of the meta-surface A_{eff} can be calculated by applying (6)

$$A_{\text{eff}} = \frac{\lambda_0^2}{4\pi} D. \tag{6}$$

Fig. 14 shows a comparison between the effective area derived from the measurements (taking into account the errors in the measurements of the gain) and the physical area of the meta-surface. When the superstrate is small (4 unit cells; A_{phy} equal to $0.18\lambda_0^2$), it can be observed that the effective area is larger than the physical one. This is an artefact effect produced by the mathematical definition of the effective area when the radiating surface is not wide enough and there are not metallic walls surrounding the antenna. This is a known phenomena described by Balanis for dipole antennas [27] p. 83. This effect can be explained through the observation of the fringing fields on the edges of the structure (see Fig. 15). However, for larger superstrates (from five to eight cells), the effective area is similar to the physical one, what means that the meta-surface is completely illuminated, i.e., a uniform illumination has been achieved. On the other hand, when the meta-surface becomes very large, the single dipole cannot excite and illuminate the whole superstrate and therefore the effective area becomes smaller than the physical one. In fact, from Fig. 14, it can be observed that the maximum area that the single dipole can illuminate is around $0.3\lambda_0^2$.

Plotting the E field on the H plane of the dipole at the resonant frequency and the Poynting vector on the radiating surface of the superstrate (see Fig. 15) the uniform illumination and the extension beyond the physical geometry of the radiated field can be observed, which is confirming the previous explanation for an effective area larger than the physical one.

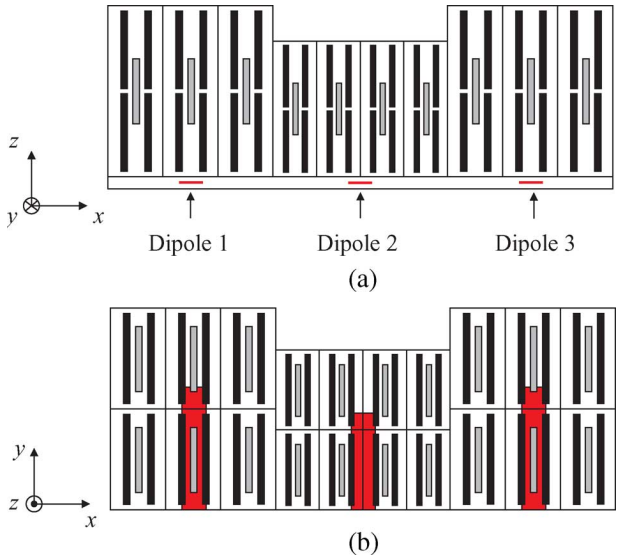

Fig. 16. Geometry of the MFAA. Notice that electromagnetic symmetry properties were applied on the xz plane, so only half of the structure is shown. Dipoles 1 and 3 are radiating at the LRF and dipole 2 at HRF. (a) Front view. (b) Top view.

IV. Multifrequency Antenna Configuration

The results obtained in the previous sections show that the physical area of the proposed structure can be used very effectively in order to enhance the radiation performance of planar antennas due to the uniform illumination of the superstrate. Other advantages of the configuration are the compactness (total thickness $\approx \lambda_0/4$), the quite symmetrical E and H-plane radiation patterns and reduced back radiation.

On the other hand, it has been observed that the unit cells are highly resonating and the field is confined on the superstrate. Although some fringing fields can appear at the edges of the structure, it is possible to place the same type of unit cell but with a different resonant frequency (same shape but different size) on both sides. In this case both unit cells will be resonating independently. By tuning two dipoles to the corresponding resonant frequency of each group of cells, a multifrequency antenna array (MFAA) can be designed with low coupling between elements.

In order to implement it, the unit cell explained in Section II has been scaled to be working at a higher frequency, around 12.5 GHz. By combining superstrates consisting of low resonant frequency (LRF) unit cells and high resonant frequency (HRF) ones, and tuning dipoles to these frequencies, the MFAA is designed. The MFAA studied is schematically depicted in Fig. 16.

The dipoles 1 are 3 are tuned to the LRF and the dipole 2 to the HRF. Due to the small dimensions of the cells, the dipoles are very close to each other ($0.23\lambda_0$ at LRF; $0.3\lambda_0$ at HRF). This potentially will allow to design compact multifrequency antennas.

By plotting the magnitude of the E-field on the H-plane of the dipoles, the low coupling between dipoles can be easily understood. When the dipoles 1 are 3 are fed [see Fig. 17(a)] the group of cells that are above them confine the power. However, the HRF cells that are in between are reflecting the power because they are not resonating, reducing at the same time the coupling

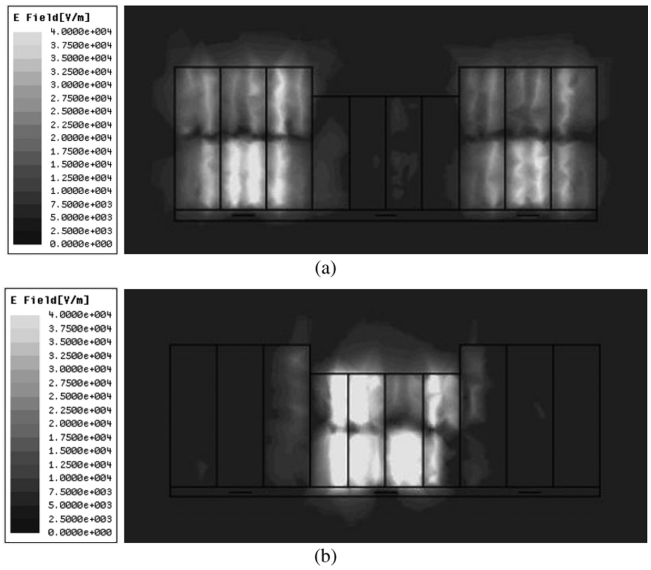

Fig. 17. Magnitude of the E field on the H-plane of the dipoles (xz plane). (a) Dipoles 1 and 3 are radiating at 10.8 GHz. (b) Dipole 2 is radiating at 12.55 GHz.

between dipoles. When the dipole 2 is active, the opposite effect occurs. Only the HRF cells transmit the power and the LRF ones that are on both sides reflect it [see Fig. 17(b)]. For distance between dipoles around 0.25 λ_0, coupling values of -20 dB have been obtained.

Plotting the H and E-plane radiation patterns (see Fig. 18), the improved performance of this MFAA can be observed. Due to the rather uniform illumination of the radiation surface (see Fig. 17), gain and aperture efficiency enhancement is obtained, keeping the low back radiation and symmetrical radiation patterns.

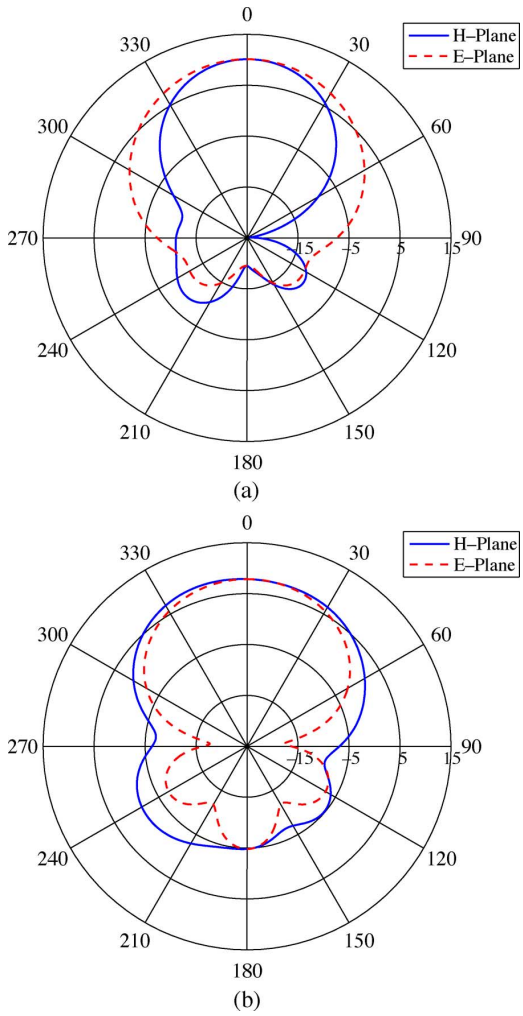

Fig. 18. H and E-plane radiation patterns (a) Dipoles 1 and 3 are radiating at 10.8 GHz. (b) Dipole 2 is radiating at 12.55 GHz.

V. Conclusion

In this paper, a novel implementation to enhance the radiation performances of a dipole antenna based on the use of meta-surfaces as superstrate has been presented. A finite uniform meta-surface has been characterized in terms of S_{11} parameter, gain, radiation pattern, radiation efficiency and effective area. Measurements of different configurations have proven an enhancement of the gain at boresight of about 3.5 $\pm$1 dB with a reduction of the H-plane endfire radiation of about 15 dB. The radiation efficiency has been calculated by means of the pattern integration technique and Wheeler cap method with efficiency values higher than 80%. For superstrates up to eight cells, the effective area was similar to the physical one, what means a uniform illumination of the meta-surface. For larger superstrates, the effective area does not increase since the maximum area that the dipole can illuminate has been estimated around $0.3\lambda_0^2$. Based on this configuration, a compact multifrequency antenna array has been simulated, showing the gain enhancement and low coupling between elements.

Acknowledgment

The authors would like to thank Prof. R. W. Ziolkowski for his helpful discussions on various aspects of this work and the support of the Wireless Communication Research Group (WiCR) of Loughborough University for their assistance with the measurements.

References

[1] Y. Sugio, T. Makimoto, S. Nishimura, and H. Nakanishi, "Analysis for gain enhancement of multiple-reflection line antenna with dielectric plates," *Trans. IECE*, pp. 80–112, Jan. 1981.

[2] N. G. Alexopoulos and D. R. Jackson, "Fundamental superstrate (cover) effects on printed circuit antennas," *IEEE Trans. Antennas Propag.*, vol. 32, pp. 807–815, Aug. 1984.

[3] D. R. Jackson and N. G. Alexopoulos, "Gain enhancement methods for printed circuit antennas," *IEEE Trans. Antennas Propag.*, vol. 33, pp. 976–987, Sep. 1985.

[4] Y. J. Lee, J. Yeo, R. Mittra, and W. S. Park, "Application of electromagnetic bandgap (EBG) superstrates with controllable defects for a class of patch antennas as spatial angular filters," *IEEE Trans. Antennas Propag.*, vol. 53, pp. 224–235, Jan. 2005.

[5] L. Zhang, H. Contopanagos, N. G. Alexopoulos, and E. Yablonovitch, "An electromagnetic bandgap resonator antenna," in *Proc. IEEE Antennas Propagation Society Int. Symp.*, Jun. 21–26, 1998, vol. 1, pp. 186–189.

[6] L. Zhang, N. G. Alexopoulos, and E. Yablonovitch, "Microstrip line fed slot antenna with pbg superstrate," in *Proc. IEEE Antennas Propagation Society Int. Symp.*, Jul. 11–16, 1999, vol. 3, pp. 1924–1927.

[7] C. Cheype, C. Serier, M. Thevenot, T. Monediere, A. Reineix, and B. Jecko, "An electromagnetic bandgap resonator antenna," *IEEE Trans. Antennas Propag.*, vol. 50, pp. 1285–1290, Sep. 2002.

[8] M. Thevenot, C. Cheype, A. Reineix, and B. Jecko, "Directive photonic-bandgap antennas," *IEEE Trans. Microw. Theory Tech.*, vol. 47, no. 11, pp. 2115–2122, 1999.

[9] B. Temelkuran, M. Bayindir, E. Ozbay, R. Biswas, M. M. Sigalas, G. Tuttle, and K. M. Ho, "Photonic crystal-based resonant antenna with a very high directivity," *J. Appl. Phys.*, vol. 87, no. 1, pp. 603–605, 2000.
[10] R. Biswas, E. Ozbay, B. Temelkuran, M. Bayindir, M. M. Sigalas, and K.-M. Ho, "Exceptionally directional sources with photonic-bandgap crystals," *J. Opt. Soc. Am. B*, vol. 18, no. 11, pp. 1684–1688, 2001.
[11] L. Leger, C. Serier, R. Chantalat, M. Thevenot, T. Monediere, and B. Jecko, "1D dielectric EBG resonator antenna design," in *Ann. Telecommun. Tome 49*, Mar.–Apr. 2004, pp. 242–260.
[12] A. Neto, N. Llombart, G. Gerini, M. D. Bonnedal, and P. de Maagt, "EBG enhanced feeds for the improvement of the aperture efficiency of reflector antennas," *IEEE Trans. Microw. Theory Tech.*, vol. 55, no. 8, pp. 2185–2193, 2007.
[13] Y. J. Lee, J. Yeo, R. Mittra, and W. S. Park, "Design of a high-directivity electromagnetic band gap (EBG) resonator antenna using a frequency-selective surface (FSS) superstrate," *Microw. Opt. Tech. Lett.*, vol. 43, pp. 462–467, Dec. 2004.
[14] R. Sauleau, *Fabry-Perot Resonators, Encyclopedia of RF and Microwave Engineering*. New York: Wiley, 2005.
[15] A. P. Feresidis, G. Goussetis, S. Wang, and J. C. Vardaxoglou, "Artificial magnetic conductor surfaces and their application to low-profile high-gain planar antennas," *IEEE Trans. Antennas Propag.*, vol. 53, pp. 209–215, Jan. 2005.
[16] A. P. Feresidis and J. C. Vardaxoglou, "High gain planar antenna using optimized partially reflective surfaces," *Proc. Inst. Elect. Eng. Microw. Antennas Propag.*, vol. 148, no. 6, pp. 345–350, 2001.
[17] S. Wang, A. P. Feresidis, G. Goussetis, and J. C. Vardaxoglou, "High-gain subwavelength resonant cavity antennas based on metamaterial ground planes," in *Proc. Inst. Elect. Eng. Microw. Antennas Propag.*, Feb. 2006, vol. 153, pp. 1–6.
[18] P. Ikonen, C. Simovski, and S. Tretyakov, "Compact directive antennas with a wire-medium artificial lens," *Microw. Opt. Tech. Lett.*, vol. 43, pp. 467–469, Dec. 2004.
[19] E. Saenz, R. Gonzalo, I. Ederra, and P. de Maagt, "High efficient dipole antennas by using left-handed superstrates," in *Proc. 13th Int. Symp. Antennas JINA*, Nov. 2004, pp. 112–118.
[20] E. Saenz, R. Gonzalo, I. Ederra, and P. de Maagt, "Transmission enhancement between rectangular waveguides by means of a left handed media," *Elect. Lett.*, vol. 41, pp. 725–727, Jun. 2005.
[21] E. Saenz, R. Gonzalo, I. Ederra, and P. de Maagt, "Application of left handed superstrates to improve radiation performances of dipole antennas," in *Proc. Eur. Microw. Association*, Mar. 2006, vol. 2, pp. 3–11.
[22] E. Saenz, I. Ederra, P. de Maagt, and R. Gonzalo, "High efficient dipole antenna with a planar meta-surface," *Elect. Lett.*, vol. 43, no. 16, Aug. 2007.
[23] D. R. Smith, W. J. Padilla, D. C. Vier, S. C. Nemat-Nasser, and S. Schultz, "Composite medium with simultaneously negative permeability and permittivity," *Phys. Rev Lett.*, vol. 84, pp. 4184–4187, May 2000.
[24] R. A. Shelby, D. R. Smith, and S. Schultz, "Experimental verification of a negative index of refraction," *Science*, vol. 292, pp. 77–79, Apr. 2001.
[25] R. W. Ziolkowski, "Design, fabrication, and testing of double negative metamaterials," *IEEE Trans. Antennas Propag.*, vol. 51, pp. 1516–1529, Jul. 2003.
[26] J. B. Pendry, "Negative refraction makes a perfect lens," *Phys. Rev Lett.*, vol. 85, pp. 3966–3969, Oct. 2000.
[27] C. A. Balanis, *Antenna Theory: Analysis and Design*, 2nd ed. New York: Wiley, 1997.
[28] H. A. Wheeler, "The radiansphere around a small antenna," in *Proc. IRE*, Aug. 1959, pp. 1325–1331.
[29] E. H. Newman, P. Bohley, and C. H. Walter, "Two methods for the measurement of antenna efficiency," *IEEE Trans. Antennas Propag.*, vol. 23, pp. 457–461, July 1975.

Elena Sáenz (S'04) was born in Viana, Navarra, Spain, in 1981. She received the M.Sc. degree in telecommunication engineering from the Public University of Navarra (UPNa), Navarra, Spain, in 2004, where she is currently working toward the Ph.D. degree.

Her doctoral research is focused on the analysis and design of metasurfaces with emphasis on their application as superstrates for antennas.

Ramón Gonzalo (S'95–M'04) was born on July 15, 1972 in Logroño, La Rioja. He received the M.Sc. and the Ph.D. degrees in "Ingeniero de Telecomunicación" (both with honors) from the Public University of Navarra (UPNa), Spain.

Since October 1995, he has been with the Antennas Group, Electrical and Electronic Engineering Department, UPNa where he is currently an Associate Professor. From September 1997 to December 1998, he was a Research Fellow to the Antenna Section in ESA-ESTEC where he was involved in the modeling and design of electromagnetic crystal devices at microwave and millimeter wave frequencies. He has been involved in more than 15 research projects, acting as Coordinator in several of them. In particular he has been Coordinator of two electromagnetic crystal projects within the framework of ESTEC contracts. He has more than 20 journal publications and 80 conference papers related to electromagnetic crystal topics. His current area of research is in the field of electromagnetic crystal structures with emphasis on space antenna applications, design of waveguide transmission lines and corrugated horn antennas.

Iñigo Ederra was born in Isaba, Navarra, Spain in 1972. He received the M.Sc. degree in telecommunication engineering from the Universidad Pùblica de Navarra, Navarra, Spain, in 1996 and the Ph.D. degree in telecommunication engineering from the Universidad Pùblica de Navarra, Navarra, Spain, in 2004.

In 1997, he joined the Microwave and Millimetre Wave Group, Universidad Pùblica de Navarra, where he was involved in the study of high-power millimeter-wave components. From 1999 to 2000, he was with the European Space Research and Technology Centre (ESTEC), ESA, Noordwijk, The Netherlands, where he was working on electromagnetic bandgap materials and their applications in the field of antennas. Since 2001, he is with the Antenna Group, Universidad Pùblica de Navarra.

His research interests are in the field of electromagnetic bandgap materials and metamaterials and their applications in microwave and millimeter wave components and antennas.

John (Yiannis) C. Vardaxoglou (M'87) received the B.Sc. degree in mathematics (mathematical physics) and the Ph.D. degree from the University of Kent at Canterbury, U.K., in 1981 and 1985, respectively.

In January 1988, he was appointed a Lecturer in Communications with the Department of Electronic and Electrical Engineering, Loughborough University of Technology, Loughborough, U.K. He was promoted to the position of Senior Lecturer in January 1992. In 1998, he was appointed Professor of Wireless Communications. He holds the Chair of Wireless Communications at Loughborough University and is the Founder of the Centre for Mobile Communications Research (CMCR). He established the Wireless Communications Research (WiCR) group at Loughborough University and he Heads the Centre for Mobile Communications Research. He has pioneered research, design and development of frequency selective surfaces (FSS) for communication systems and has commercially exploited a number of his innovations. He has been active in the analysis and design of small low specific absorption rate (SAR) material loaded antennas for mobile telephony and electromagnetic band gap (EBG) structures for subsystem applications. His current research interests include array antennas, FSS, radomes, leaky wave resonant antennas, optical control of microwaves and devices, periodic surfaces and EBG/AMC/LH materials, and material-loaded mobile telephone antennas. He has served as a consultant to various industries, holds three patents and is the Technical Director of Antrum, Ltd. He has published over 130 refereed journals and conference proceeding papers and has written a book on FSS.

Dr Vardaxoglou is currently the Chairman of the Executive Committee of the Antennas and Propagation Professional Network of the Institution of Engineering and Technology (IET), London, U.K., and he Chairs the IEEE's Distinguish Lecturer Program of the Antennas and Propagation Society. He Chairs the Executive Committee of Metamorphose, EU FP6 Network of Excellence of Metamaterials. He chaired the 1st and 2nd Institution of Electrical Engi-

neers's (IEE) Antenna Measurements and SAR (AMS'02 and AMS'04) Conferences and has been on the organizing committee of the 2001 and 2003 IEE International Conferences on Antennas and Propagation. He was the General Chair of the 1st and 2nd Loughborough Antennas and Propagation Conference (LAPC'05).

Peter de Maagt (S'88–M'88–SM'02–F'07) was born in Pauluspolder, The Netherlands, in 1964. He received the M.Sc. and Ph.D. degrees from Eindhoven University of Technology, Eindhoven, The Netherlands, in 1988 and 1992, respectively, both in electrical engineering.

He is currently with the European Space Research and Technology Centre (ESTEC), European Space Agency, Noordwijk, the Netherlands. His research interests are in the area of millimeter and submillimeter-wave reflector and planar integrated antennas, quasi-optics, electromagnetic bandgap antennas, and millimeter- and sub-millimeter-wave components.

Dr. de Maagt was co-recipient of the H. A. Wheeler Award of the IEEE Antennas and Propagation Society for the Best Applications Paper of the year 2001. He was granted a European Space Agency Award for Innovation in 2002. He was corecipient of the Loughborough Antennas and Propagation Conference (LAPC) 2006 and the International Workshop on Antenna Technology (IWAT) 2007 Best Paper Award.